Annals of Nuclear Energy 77 (2015) 425–435

Contents lists available at ScienceDirect

Annals of Nuclear Energy

journal homepage: www.elsevier.com/locate/anucene

Development of a sub-channel code for liquid metal cooled fuel assembly

X.J. Liu [a,*], N. Scarpelli [a,b]

[a] School of Nuclear Science and Engineering, Shanghai Jiao Tong University, 800 Dongchuan Road, Shanghai 200240, China
[b] Department of Energy, Polytechnic University of Turin, School of Engineering, Corso Duca degli Abruzzi 24, Torino 10129, Italy

ARTICLE INFO

Article history:
Received 6 August 2014
Received in revised form 23 October 2014
Accepted 24 October 2014
Available online 17 December 2014

Keywords:
Liquid metal reactor
Sub-channel analysis
Code development
Verification and validation

ABSTRACT

Extensive study has been carried out for liquid metal cooled reactors (LMR). One of the challenges for the design of LMR is to keep the cladding temperature below the design limit. Thus, accurate prediction of coolant and fuel cladding temperature is highly required. In this study, a sub-channel analysis code COBRA-LM is developed for thermal-hydraulic analysis of liquid metal reactor. Based on COBRA-IV code, the development work of COBRA-LM can be divided into two steps. Firstly, Sodium and Lead–Bismuth properties calculation is introduced; secondly, pressure drop models, turbulent mixing models and heat transfer correlations are investigated and implemented into the code. Furthermore, verification and validation study of the new developed COBRA-LM code is performed. The ORNL-19 pin tests are chosen to assess the code's capability. Comparisons are performed to demonstrate the accuracy of the code by the results of CFX, MATRA-LMR and ORNL-19 test data. According to the results, it can be concluded that a reliable tool for sub-channel analysis of LMR is developed, model recommendation is also given for future study. Finally, an analysis for PHENIX reactor is simulated by COBRA-LM code.
© 2014 The Authors. Published by Elsevier Ltd. This is an open access article under the CC BY-NC-ND license (http://creativecommons.org/licenses/by-nc-nd/3.0/).

1. Introduction

In the framework of Generation IV International Forum (GIF), technology goals were set for the middle-long term of nuclear reactor projects. In order to achieve diverse objectives among which the waste minimization, three types of fast reactors (Gas-cooled Fast Reactor, Lead-cooled Fast Reactor, Sodium-cooled Fast Reactor) were considered. Liquid metals are foreseen to be used as coolants for GEN IV fast reactors, as well as for Accelerator Driven Systems. Thanks to the operating experience already gained in the past years, one possible mid-term available fast reactor seems to be Sodium-cooled Fast Reactor.

Due to the higher operating temperatures of fast reactors (outlet temperature over 500 °C) with respect to LWRs, many constraints about corrosion phenomena by liquid metals are posed. In order to meet economical and safety considerations, temperature distributions are key-point in the design of liquid metal reactor cores. Several design limits are concerning fuel, cladding and coolant temperatures, thus an accurate prediction of the thermal-hydraulic behavior of the core assemblies is an essential prerequisite to reactor design. Therefore, considerable experimental and theoretical studies are necessary to acquire a detailed knowledge of LMR assemblies and fuel pins conditions (Gen IV Roadmap, 2002). In the LMR design, wire wrap spacer is adopted to enhance the coolant mixing flow between sub-channels and to maintain the cooling geometry by prevention the fuel rod contacting adjacent rods.

Nowadays, the sub-channel analysis approach is usually adopted to evaluate the local thermal-hydraulic behavior of the fuel assemblies. In a sub-channel analysis code, mass, momentum and energy conservation equations are modeled and solved together with initial and boundary conditions (Steward et al., 1977). In the past, great effort has been devoted to develop reliable sub-channel analysis tools for thermal-hydraulic analysis providing coolant temperature fields in the bundle, e.g., MATRA-LMR, SLTHEN, SABRE4 and COBRA-WC.

MATRA-LMR (Kim et al., 2002) was developed at Korea Atomic Energy Research Institute (KAERI) by adaptation of MATRA to sodium coolant reactor. SABRE4 (Dobson and O'Neill, 1992) is widely used in the UK; it is a 3-D sub-channel code designed to predict the thermal-hydraulics of a sodium fast reactor fuel assembly. SLTHEN is a modified version of ENERGY, specifically developed for LMR (e.g., sodium fast reactor), providing improved computational efficiency and simplified energy equation mixing model (Yang, 1997). COBRA-WC is derived from COBRA-IV to analyze liquid metal fast breeder reactor assembly transients. It was

* Corresponding author.
E-mail address: xiaojingliu@sjtu.edu.cn (X.J. Liu).

http://dx.doi.org/10.1016/j.anucene.2014.10.030
0306-4549/© 2014 The Authors. Published by Elsevier Ltd.
This is an open access article under the CC BY-NC-ND license (http://creativecommons.org/licenses/by-nc-nd/3.0/).

Nomenclature

C_P	specific heat/(J kg^{-1} K^{-1})
D	diameter/m
D_e	equivalent diameter/m
F	correction factor/–
f	friction factor/–
G	mass flux/(kg m^{-2} s^{-1})
H	wire wrap pitch/m
LEB	lead-bismuth eutectic
LMR	liquid metal cooled reactors
LWR	light water reactor
Nu	Nusselt-number/–
P	pitch of the rod/m
p	pressure/MPa
Pe	Peclet number/–
Pr	Prandtl-number/–
q''	heat flux/(W m^{-2})
Re	Reynolds number
S	gap between two adjacent sub-channels/m
SSG	Speziale–Sarkar–Gatski Reynolds stress model
T	temperature/°C
ω'	turbulent mixing flow rate/(kg/m-s)
V	velocity/(m/s)
β	turbulent mixing coefficient/–
σ	surface tension/(N m^{-1})
λ	thermal conductivity/(W m^{-1} K^{-1})
μ	dynamic viscosity/(Pa s)
ρ	density/(kg m^{-3})

Subscripts

ave	average
B	boiling point
in	inlet
M	melting point
out	outlet
W	wall

specifically developed to analyze a core flow coastdown to natural circulation cooling. The detailed information about COBRA-WC code and the difference between COBRA-IV and COBRA-WC can be found in the report from Pacific Northwest Laboratory (George et al., 1980). However, as pointed out in a recent paper (Wu et al., 2013), there are still some limitations for the current sub-channel codes, e.g., limitation for the calculation speed and number of the fuel rod and sub-channels. Moreover, it should be noted that an intensive investigate of various thermal hydraulic models in sub-channel code, e.g., heat transfer and mixing correlations are required to recommend proper models for LMR simulation. Therefore, a model sensitivity analysis for sub-channel code is also needed.

In the frame of this study, the development of a sub-channel analysis code COBRA-LM for liquid metal reactors is presented. The sub-channel code COBRA-IV was adapted to deal with sodium and lead-bismuth eutectic cooled bundles, and confirmed by the benchmark analysis. The results achieved in this paper provide a reliable tool for the sub-channel analysis of the LMR, some model recommendations are also given for the future study.

2. Development of COBRA-LM

The development of the sub-channel code consists in the adaptation of a reference code toward the analysis of liquid metals application in nuclear reactors. As mentioned in the introduction, COBRA-IV-I (Steward et al., 1977) is the reference code for this purpose. While COBRA-IV-I deals with water in PWRs, COBRA-LM aims to describe the thermal-hydraulic behavior of liquid metal flows in reactor bundles. Therefore, the properties of the coolant and the models related to flowing and heat transfer of LMR should be adapted. Thus, this study entailed the modification of following issues:

- Properties of the liquid metal coolant
- Pressure drop models for liquid metal
- Turbulent mixing models for liquid metal
- Heat transfer correlations for liquid metal

In order to develop a both reliable and flexible tool open to improvements, a wide range of models are analyzed in this paper. The following subsections describe in detail the modifications to the reference code.

2.1. Liquid metal properties

Intensive studies have been performed in different countries aiming at a better understanding of liquid metals properties needed for design and safety analysis of the nuclear installations. The thermo-physical properties of these coolants were measured in many laboratories, but mainly at atmospheric pressure and at relatively low temperatures (except for sodium). In general, the reliability of data is satisfactory, especially for sodium.

For the analysis of liquid metal cooled fuel assemblies, several modifications to COBRA-IV-I were necessary as the original code does not allow direct calculation of the thermo-physical properties of liquid metals. In fact, COBRA-IV-I is provided with water properties in tabular form. A review and compilation of data available in open literature for the main thermo-physical properties of liquid metal (sodium and lead–bismuth eutectic: LBE) is provided by Sobolev (2010). Table 1 summarizes the main property of these two liquid metal. Eventually, a full set of both sodium and LBE property correlations was implemented in COBRA-LM.

From the correlation of the specific heat, it is possible to find an equation for the enthalpy increment, taking the melting point as reference value. Thus, the specific enthalpy per unit mass as a function of temperature at the given pressure is obtained by integration of the isobaric specific heat capacity over temperature, as illustrated in Eq. (1):

$$h(T,p) = h(T_M,p) + \int_{T_M}^{T} C_p(T,p)dT \tag{1}$$

2.2. Pressure drop models

Liquid metal reactors fuel assembly presents tight arrangement of thin fuel pins together with hexagonal geometry. This design feature can provide a high heat transfer coefficient for liquid metals. However, proper spacing between the fuel pins is necessary; therefore, helical wire-spacers are frequently used. This implies that a suitable pressure drop correlations for wire-wrapped rod bundles should be implemented into the sub-channel code.

Table 1
Correlations for the liquid metal calculation (Sobolev, 2010).

Property	Unit	Sodium	LBE
Melting point	K	$T_M = 371.0$	$T_M = 398.0$
Boiling point	K	$T_B = 1155.0$	$T_B = 1927.0$
Surface tension	N/m	$\sigma = (231 - 0.0966 \cdot T) \times 10^{-3}$	$\sigma = (448.5 - 0.08 \cdot T) \times 10^{-3}$
Density	kg/m^3	$\rho = 1104 - 0.235 \cdot T$	$\rho = 11{,}065 - 1.293 \cdot T$
Isobaric specific heat	J/kg K	$C_p = -3.001 \times 10^6 \cdot T^{-2} + 1658 - 0.8479 \cdot T + 4.454 \times 10^{-4} \cdot T^2$	$C_p = 164.8 - 3.94 \times 10^{-2} \cdot T + 1.25 \times 10^{-5} \cdot T^2 - 4.56 \times 10^5 \cdot T^2$
Dynamic viscosity	Pa s	$\ln \mu = \frac{556.835}{T} - 0.3958 \ln T - 6.4406$	$\mu = 4.94 \times 10^{-4} \cdot \exp(\frac{754.1}{T})$
Thermal conductivity	W/m K	$\lambda = 104 + 0.047 \cdot T$	$\lambda = 3.284 + 1.617 \times 10^{-2} \cdot T - 2.305 \times 10^{-6} \cdot T^2$

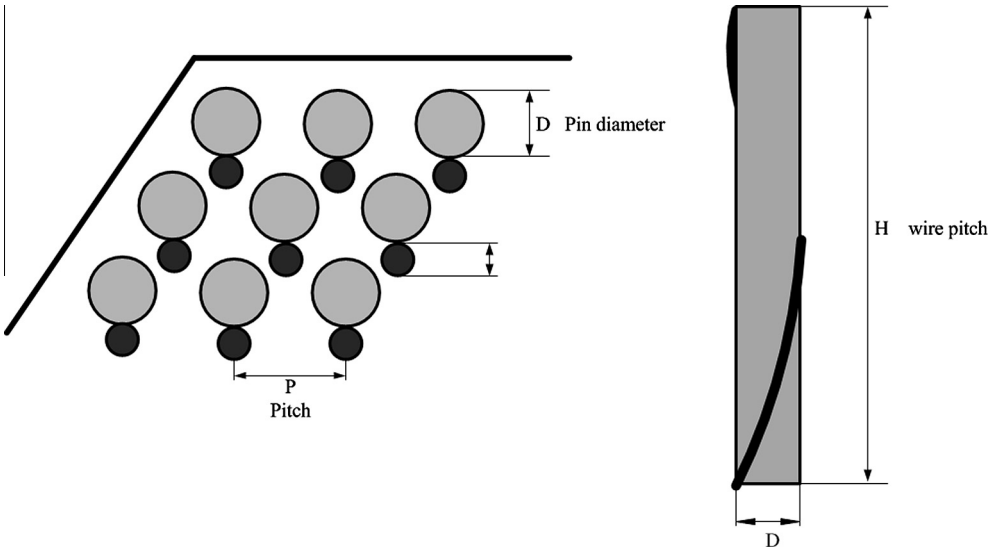

Fig. 1. Detailed of sub-channels and wire wrap geometry.

Because of the complex geometry due to the wire wraps (as shown in Fig. 1), the simple models, of which the reference sub-channel code is adopted, are not sufficient to characterize the flow behavior of LMR subassemblies. An accurate prediction of the pressure drop is needed, thus input parameters concerning the friction term must be provided through empirical correlations. The pressure drop in the fuel pin region is a key point for sub-channel analysis since it is affecting both the flow distributions and the heat transfer conditions.

McAdams (1942) proposed a correlation (Re $\geqslant$ 3000) for the wall frictional coefficient for turbulent flow,

$$f = \frac{0.184}{\mathrm{Re}^{0.2}} \tag{2}$$

However, it is a very simple model and it does not account for the effect from wire wrap. An extensive study on the more complex empirical models available in literature lead us to present the following.

2.2.1. Novendstern model

Novendstern (1972) developed a semi-empirical model suitable for hexagonal wire-wrapped fuel pin assemblies. In this model the wire wrap is taken into account by means of an effective friction factor. The pressure drop is obtained using Blasius correlation, i.e., Eq. (3), for smooth pipes. Then, the correlation involves a multiplication factor M to account for the wire spacers.

$$f_{\mathrm{smooth}} = \frac{0.3164}{\mathrm{Re}^{0.25}} \tag{3}$$

$$M = \left[\frac{1.034}{(P/D)^{0.124}} + \frac{29.7(P/D)^{6.94}\mathrm{Re}^{0.086}}{(H/D)^{2.239}}\right]^{0.885} \tag{4}$$

Using the flow conditions for the central sub-channel, the pressure drop is obtained by

$$\Delta p = M f_{\mathrm{smooth}} \frac{L}{D_e} \frac{\rho V^2}{2} \tag{5}$$

In Eq. (4), the geometry of the problem is defined by the rod pitch to diameter ratio P/D and by the wire wrap pitch to rod diameter ratio H/D. The geometry poses limits of application for the model: $2600 \leqslant Re \leqslant 200{,}000$, $1.06 \leqslant P/D \leqslant 1.42$, $8.0 \leqslant H/D \leqslant 96.0$.

2.2.2. Rehme model

Rehme (1972) introduced an effective velocity to take into account the swirl flow velocity caused by the presence of the wire wraps:

$$F = \left(\frac{V_{\mathrm{eff}}}{V}\right)^2 = (P/D)^{0.5} + \left[7.6\frac{D + D_w}{H}(P/D)^2\right]^{2.16} \tag{6}$$

where D_w is the wire wrap diameter. A modified friction factor is presented as follows:

$$f' = \frac{f}{F}\frac{P_{wt}}{P_{wb}} = \frac{64}{\mathrm{Re}'} + \frac{0.0816}{\mathrm{Re}'^{0.133}} \tag{7}$$

where P_{wb} is the wetted perimeter of the rod bundle and P_{wt} is the total wetted perimeter. The modified Reynolds number is proposed below:

$$\mathrm{Re}' = \mathrm{Re}\sqrt{F} \tag{8}$$

Applicability range: $1000 \leqslant \mathrm{Re} \leqslant 300{,}000$, $1.125 \leqslant P/D \leqslant 1.417$.

2.2.3. Cheng–Todreas simplified model

Cheng and Todreas (1986) developed their sub-channel friction factor model using an extensive amount of experimental data. In this correlation, the bundle friction factor and the sub-channel friction factors for each sub-channel are derived. A simplified form of the original model is also available. From experimental results, the difference between the original and the simplified correlations is less than 1% (Chun and Seo, 2001). In the frame of this study, the simplified model was adopted. The relations are shown below:

$$C_f = \{0.8063 - 0.9022 \cdot \log(H/D) + 0.3526 \cdot [\log(H/D)]^2\}(P/D)^{9.7}(H/D)^{1.78-2(P/D)} \quad (9)$$

$$f = \frac{C_f}{\mathrm{Re}^{0.18}} \quad (10)$$

Applicability range: $400 \leqslant \mathrm{Re} \leqslant 100{,}000$, $1.067 \leqslant P/D \leqslant 1.35$, $4.0 \leqslant H/D \leqslant 52.0$.

The model shown above have been implemented in the code and it can be selected in the input deck along with the other models. Fig. 2 depicts a comparison of the implemented pressure drop models depending on the Reynolds number (with the $P/D = 1.2432$ and $H/D = 52.1918$). It can be seen that with increasing the Reynolds number, a well agreement is achieved among various models.

2.3. Turbulent mixing characterization

In order to obtain the flow and temperature distributions throughout the sub-channels, the conservation equations are modeled and solved. It is of great importance to simulate a local structure of inter-channel exchange. Therefore, the inter sub-channel mixing phenomenon due to crossflow needs to be modeled very precisely to improve the accuracy of the code.

The mixing phenomenon consists of two terms: the forced mixing and the natural one. In the natural mixing term we can still point out two different contributions: a diversion flow term and a turbulent term. The first is modeled by distributed resistance analysis and axial pressure drop correlations. The turbulent mixing, instead, is a result of the eddy motion of the fluid across the gap between the sub-channels and it enhances the exchange of momentum and energy with no net mass transfer. In sub-channel codes such as COBRA-IV and MATRA, the effects of turbulent mixing are taken into account in the axial momentum equation and in the energy conservation equation (Jeong et al., 2007). The turbulent mixing flow rate ω' can be expressed by Eq. (11):

$$\omega' = \beta \cdot S_{ij} \cdot G_{ij} \quad (11)$$

Sub-channel codes determine the turbulent mixing flow rate ω', defined per unit length between sub-channels i and j as shown in Eq. (11). S_{ij} is the gap between two adjacent sub-channels, G_{ij} is the mean flow rate of the two sub-channels, while β is the turbulent mixing coefficient.

In literature (Jeong et al., 2007), correlations dealing with turbulent mixing coefficient in rod bundles are available in large extent. Nevertheless, there is a variety of definitions of mixing parameters and a large discrepancy of results. The most general form of turbulent mixing correlation is the one providing a value for the β coefficient as a function of Reynolds number for a particular geometry fixed by the gap width to rod diameter ratio S/D. This β coefficient is considered to be the same as the gap Stanton number St_g (Jeong et al., 2007).

In the modification of the sub-channel code, the implementation of turbulent mixing correlations for the β coefficient was carried out. Table 2 summarizes most of the current correlations. The data show considerable scattered characteristics following the variety of both geometry and Reynolds number range related to the experiments, as indicated in Fig. 3. Thus, the applicability range of existing correlations is limited to specified geometries and coolants. More complex equations including hydraulic diameter or gap width, e.g., the Rogers-Tahir model, does not imply a better characterization of the turbulent mixing. This was assessed by calculations performed preliminarily in order to evaluate the models.

Recently, Cheng and Tak (2006) proposed a correlation based on CFD analysis of lead–bismuth eutectic flows in both triangular and square lattices. As shown in Eq. (12), the coefficient c depends on the geometry of the channel and it is slightly varying with the Reynolds number. For a triangular lattice with S/D equal to 0.5, it was found that the mixing coefficient is about 0.02.

$$\beta = 0.2 \cdot c \cdot Re^{-0.125} \quad (12)$$

Table 2
Correlations selected for turbulent mixing coefficient (Jeong et al., 2007; Cheng and Tak, 2006).

Model	S/D	β
Galbraith-Knudsen	0.028	$0.001571\mathrm{Re}^{0.23}$
	0.063	$0.002871\mathrm{Re}^{0.12}$
	0.228	$0.005999\mathrm{Re}^{0.01}$
Rogers-Rosehart	–	$0.005(D_e/S)\mathrm{Re}^{-0.1}$
Castellana	0.334	$0.027\mathrm{Re}^{-0.1}$
Cheng-Tak	–	$0.2 \cdot c \cdot \mathrm{Re}^{-0.125}$
Rogers-Tahir	–	$0.005(D_e/S)(S/D)^{0.105}\mathrm{Re}^{-0.1}$

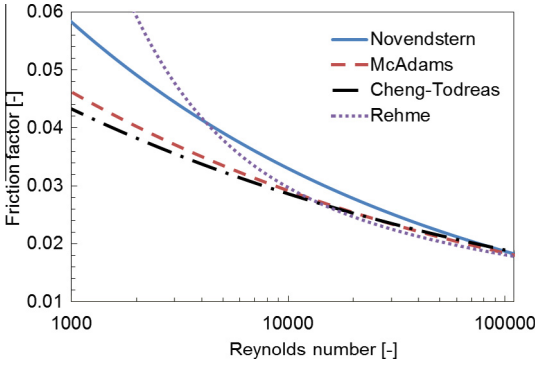

Fig. 2. Friction factor versus Reynolds number for selected pressure drop models.

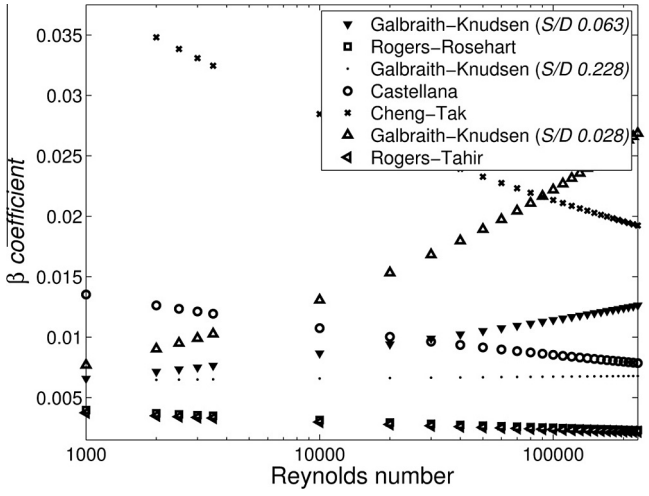

Fig. 3. Comparison of some turbulent mixing correlations.

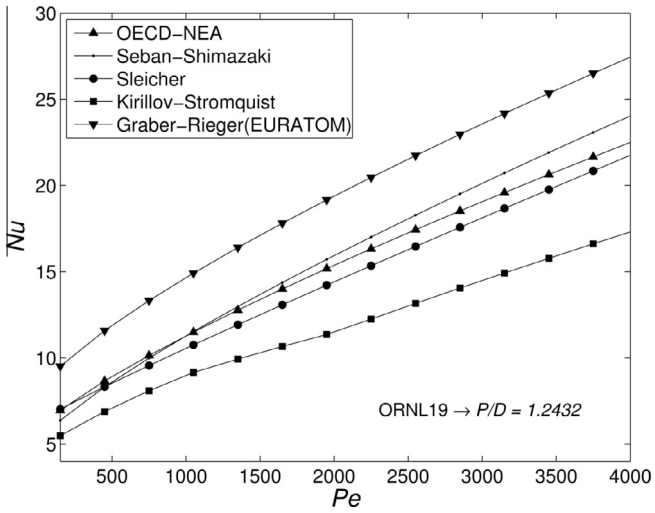

Fig. 4. Comparison of implemented heat transfer models (P/D = 1.2432, sodium at 420 °C).

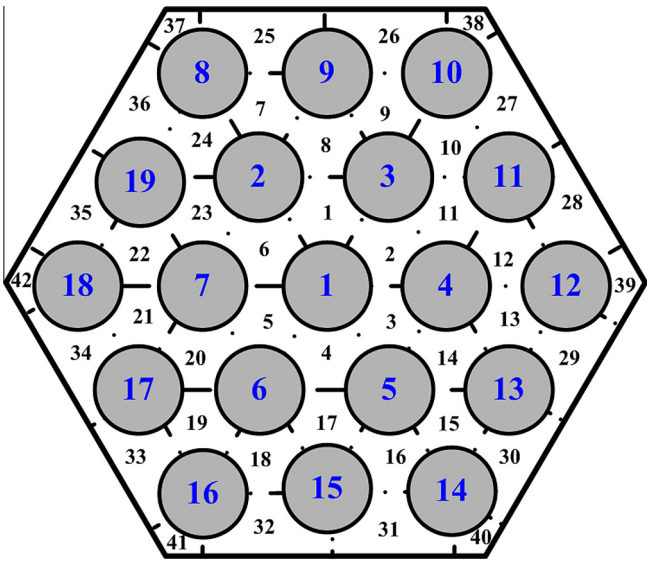

Fig. 5. Sub-channel numbering scheme (Fontana et al., 1974).

The turbulent mixing of a heavy liquid metal such as LBE is expected to be similar to the one of sodium. Therefore, it brought us to implement the Cheng-Tak model.

The main purpose of this paper is to highlight the importance of turbulent mixing data for an accurate predictability of the sub-channel code, rather than looking for the best correlation for the selected rod bundle configuration. As it will be presented later, the turbulent mixing strongly affects the flow and temperature distributions, therefore it must be considered as a fundamental parameter for the thermal-hydraulic analysis of the sub-channels.

2.4. Heat transfer correlations

In the open literature, a large number of correlations for liquid metals are available. Most of them take an expression similar to the following equation,

$$Nu = A + B \cdot Pe^n \tag{13}$$

where A, B and n are a constants. Liquid metals heat transfer is obviously different from that of water. The Prandtl number has an important role and in the case of liquid metals it is much lower because of the high thermal conductivity. Low Prandtl number means that heat transfer is conduction-dominated; the heat is transferred easily into the coolant with relatively little resistance.

As far as the sodium is concerned, both viscosity and specific heat are not so much different from the water, while the thermal conductivity is 100 times bigger. For a sub-channel analysis to be as accurate as possible, specific correlations should be tailored to the conditions of the rod bundle. In the frame of COBRA-LM, the switch for selecting the heat transfer coefficient through different models has been implemented.

Fig. 4 presents the heat transfer correlations listed in Table 3. From Fig. 4, Graber model presents a higher estimation of Nusselt number, while Kirillov-Stromquist gives the lowest value. In literature, researchers suggest that, for heat transfer analysis of heavy liquid metals like LBE, Sleicher model was recommended because of the reasonable boundary condition of the correlation is derived (Cheng et al., 2004). So the Sleicher correlation is selected for the reference sub-channel analysis for liquid metals.

3. Code validation

When the code development is finished, the code should be validated or verified by the experimental data or benchmark calculation to demonstrate its feasibility and applicability. In order to validate COBRA-LM, the ORNL 19-pin tests (Fontana et al., 1974) together with the results obtained through MATRA-LMR (Kim et al., 2002) are selected. The accuracy of the calculation is also checked through an energy balance calculation, which appeared to be consistent with the output data.

3.1. Test description

ORNL 19-pin tests were performed in the fuel failure mockup (FFM), a large high temperature sodium facility built specifically for testing simulated LMR fuel rod bundles at design thermal-hydraulic conditions. Rod bundle 2A is the configuration which our simulation was referred to. The related fuel rod had a 53.34 cm heated length, starting 40.64 cm from the bottom and it is cooled by liquid sodium. The geometry and sub-channel distribution is shown in Fig. 5. The detailed input data are summarized in Table 4.

Table 3
Correlations selected for heat transfer coefficient.

Model	Correlation	Boundary conditions/applicability range
OECD-NEA (2007)	$Nu = 5.75 + 0.022Pe^{0.8}$	$6 \times 10^3 < Re < 6 \times 10^4$
Seban and Shimazaki (1951)	$Nu = 5.0 + 0.025Pe^{0.8}$	T_w = constant
Kirillov and Ushakov (2001) and Stromquist and Boarts (1953)	$Nu = A + 0.018Pe^{0.8}$	$Pe \leqslant 1000 \rightarrow A = 4.5$ $1000 < Pe < 2000 \rightarrow A = 5.4 - 9 \cdot 10^{-4} \cdot Pe$ $Pe \geqslant 2000 \rightarrow A = 3.6$
Sleicher (Cheng et al., 2004)	$Nu = 6.3 + 0.0167Pe^{0.827}\,\mathrm{Pr}^{0.808}$	q'' = constant
Gräber and Rieger (1972)	$Nu = 0.25 + 6.2\frac{P}{D} + (0.032\frac{P}{D} - 0.007) \cdot Pe^{0.8-0.024\frac{P}{D}}$	$1.2 \leqslant P/D \leqslant 2.0$ $150 \leqslant Pe \leqslant 4000$

Table 4
Geometry data for ORNL FFM 2A 19 pin test (Fontana et al., 1974).

	Value
Geometry data	
Rod diameter (mm)	5.84
Pitch to diameter ratio (–)	1.243
Wire wrap diameter (mm)	1.42
Wire wrap pitch (mm)	304.8
Total length (mm)	1016.0
Heating length (mm)	533.4
Operation data	
System pressure (Pa)	10132.0
Inlet temperature (°C)	315
Inlet mass flow (kg/s)	3.08
Average rod power(W)	16,975
Axial power distribution	Uniform
Radial power distribution	Uniform

Several runs were performed during the experimentation with FFM bundle 2A using various flow and power conditions. In this paper, the high power and high flow case was selected to simulate. With regards to the computation accuracy and taking into account computing time and storage, the 70 axial nodes was adopted for the COBRA-LM simulation of ORNL 19-pin tests.

A reference case was introduced by selecting a basic set of models for the sub-channel analysis code. The normalized temperature factor defined in Eq. (14) is chosen for validation purpose. As mentioned before, the coolant temperature in each sub-channel is not dependent on the heat transfer correlations since its distribution is computed through energy conservation models. Therefore, the heat transfer model does not affect this temperature rise factor calculation

$$\text{Normalized temperature factor} = \frac{T_{out,sub} - T_{in}}{T_{out,ave} - T_{in}} \tag{14}$$

In Eq. (14), where the subscript *out*, *in*, *ave*, *sub* stand for outlet, inlet, average and specified sub-channel respectively.

The following models are selected in COBRA-LM reference case to perform the benchmark calculation:

- Cheng-Todreas pressure drop model
- Galbraith-Knudsen ($S/D = 0.228$) correlation for turbulent mixing coefficient The reason behind the choice of the Cheng-Todreas model for the reference case lied in past research available in literature, such as the investigation of Chun and Seo (2001), which proved the reliability of this model.

As for the turbulent mixing coefficient, the correlation of Galbraith-Knudsen ($S/D = 0.228$) was selected firstly. The reason for this choice was the S/D value similar to the one of the ORNL 19-pin test. Once again, it is important to stress that these models were both derived from experiments with water flows, therefore the geometry was not the most important deciding factor.

3.2. Comparing to CFX simulation

Before comparing to the experimental data, a CFX simulation is performed for 1/12 bundle in Fig. 5. As shown in Fig. 6, the total mesh number in the calculation domain is 2,455,080, and the turbulent model applied is SSG (Speziale–Sarkar–Gatski) model. The properties of the sodium in this calculation are derived from Table 1. Due to simplification purpose, the heating rods and wire wrap are not simulated. A uniform inlet velocity and constant heat flux boundary is used to simulate the inlet flow and heating. The geometry and operation condition is the same as that in Table 4.

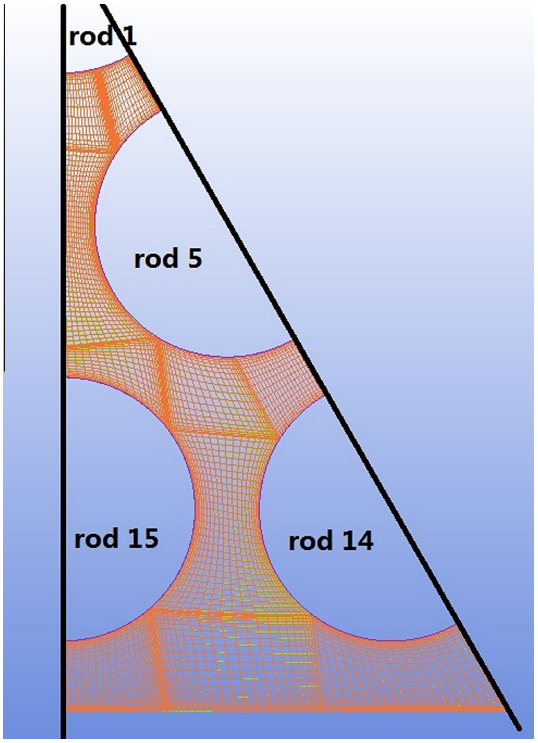

Fig. 6. Mesh in the CFX calculation domain.

Fig. 7 shows the normalized temperature comparison between the COBRA-LM and CFX simulation. Good agreement is achieved and it demonstrates the feasibility and applicability of the new developed code COBRA-LM. It should be noted that the normalized outlet temperature in each typical sub-channel deviates from that in the experiment. This is caused by the omission of the wire wrap in both CFX and sub-channel simulations.

3.3. Comparing to the experimental data

The results for the validation procedure are presented in terms of normalized temperatures at the end of the heated length. Fig. 8 depicts temperature profiles in different sub-channels among calculations by COBRA-LM reference case, MATRA-LMR and the experimental data.

From Fig. 8 it can be seen that the temperature distributions obtained by code COBRA-LM shows a similar behavior with MATRA-LMR. It predicts the experiment data within a maximum 15% deviation. Both codes give an over-estimation for the normalized temperature, except for the corner-type sub-channel 41.

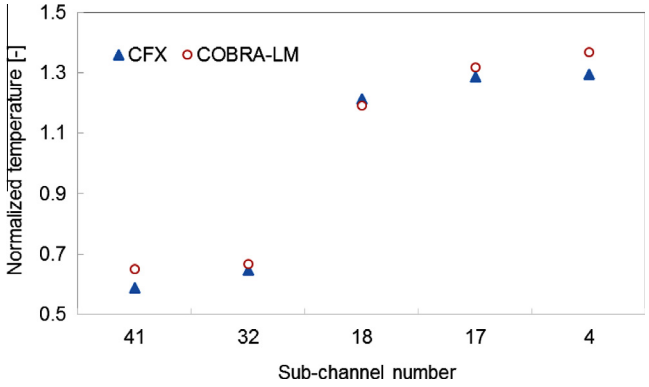

Fig. 7. Normalized temperature profile between CFX and COBRA-LM.

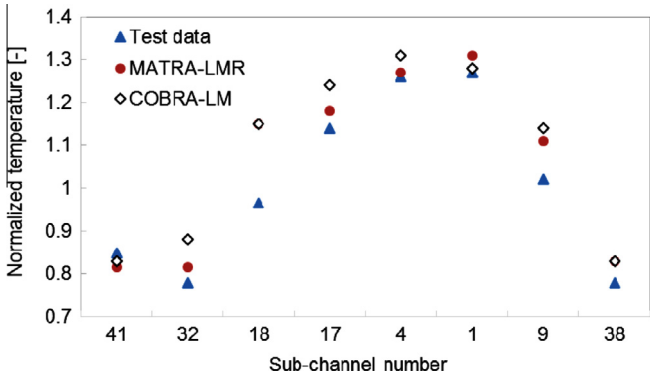

Fig. 8. Normalized temperature profile simulation v.s. data.

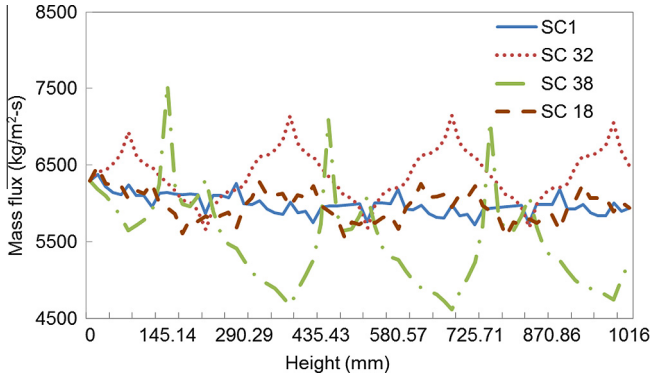

Fig. 9. Mass flux profile for typical sub-channel.

Fig. 9 shows the mass flux in typical sub-channels i.e., interior, side, and corner sub-channels. It can be concluded that the mass flux in side and corner sub-channels (SC32, SC38) presents a stronger variation than that in the center sub-channels due to the existence of the wire wrap. Considering the results achieved in Figs. 7 and 8, it has to be pointed out the importance of modeling the wire wraps and the turbulent mixing for an accurate prediction of the coolant temperature. Furthermore, the pressure drop model plays an important role of the mass flow distribution in the bundle. Therefore, the effect of the thermal-hydraulic models, i.e. pressure drop and turbulent mixing, on the normalized temperature profile, are selected to discuss during the sensitivity analysis.

4. Sensitivity analysis

A reference case for COBRA-LM is established and the temperature distribution within the rod bundle is obtained. In this section, the assessment of different sets of models for the sub-channel analysis code is carried out. By varying the combination of thermal-hydraulic models, it is possible to evaluate the mutual influence towards the results. Thus, an open calculation is performed in order to highlight the set of pressure drop, turbulent mixing and heat transfer correlations which provides the closest results to the benchmark data. During this study, considerations regarding the performance of the different models and their influence upon the output parameters are emphasized.

4.1. Normalized temperature

In this section, 20 cases with various sets of pressure drop, turbulent mixing model are performed to investigate the model effect on normalized temperature profile in sub-channels. Figs. 10–13

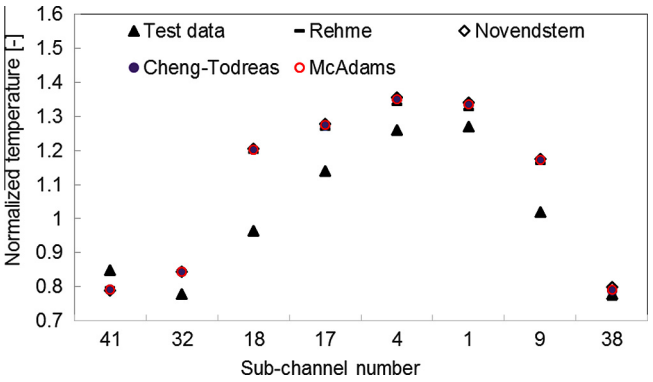

Fig. 10. Normalized temperatures at the end of the heated length (turbulent mixing model Castellana).

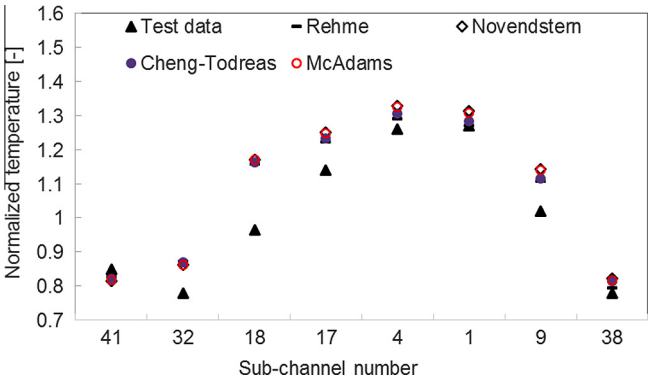

Fig. 11. Normalized temperatures at the end of the heated length (turbulent mixing model Kim-Chung).

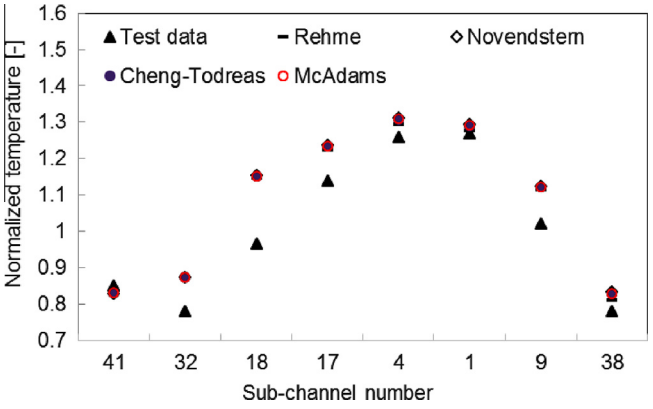

Fig. 12. Normalized temperatures at the end of the heated length (turbulent mixing model Galbraith-Knudsen *S/D* 0.228).

show the normalized temperature distribution for the pressure models used in COBRA-LM code with ORNL 19-pin test high flow case. The pressure drop strongly affects the estimation of the temperatures among the sub-channels; it is very important to evaluate the accuracy of the correlations, keeping the turbulent mixing coefficient fixed.

Novendstern model generally overestimate the normalized temperatures and McAdams model is predicting slightly smaller normalized temperatures than the Novendstern model. Both Cheng-Todreas and Rehme correlations provides more accurate results. Castellana model for turbulent mixing leads to a more pre-

cise prediction of the outermost sub-channels temperature, but large overestimation for central sub-channels. From Fig. 14, it can be seen that both Cheng-Tak and Galbraith-Knudsen turbulent mixing models present better predictions for the interior sub-channels. On the other hand, these two models flat the temperature distribution and contribute to a raise of temperature in the side channels.

After the analysis of the combinations of models, it is concluded that the pressure drop is crucial to predict the temperatures of the interior sub-channels in some cases (in Fig. 11), while the turbulent mixing is extensively affecting the outer sub-channels (i.e., side and corner sub-channel). In addition, the turbulent mixing is flattening the temperature profile since the exchange of energy between the channels is enhanced. The bigger value of the turbulent mixing coefficient, the smaller value of the hot channel factor would be. This point was stressed in the study of the rod temperatures.

According to the square root of the variances between the normalized temperatures of the test data and the ones provided by COBRA-LM, it was possible to assess the different sets of models involved. This criterion and compared results provide us the following combination of thermal-hydraulic correlations as the best one in terms of temperature prediction with regards to the ORNL 19-pin test (it also can be seen from Fig. 14):

- Rehme pressure drop model
- Cheng-Tak correlation for turbulent mixing coefficient Although the error between the results obtained by this code and experimental data is the smallest, it should be pointed out that Rehme model gives the lowest normalized temperatures. Cheng-Todreas model coupled with Cheng-Tak correlation showed a slightly lower accuracy of the results in most of sub-channel but better estimation of the temperature in the hot channels (center channel).

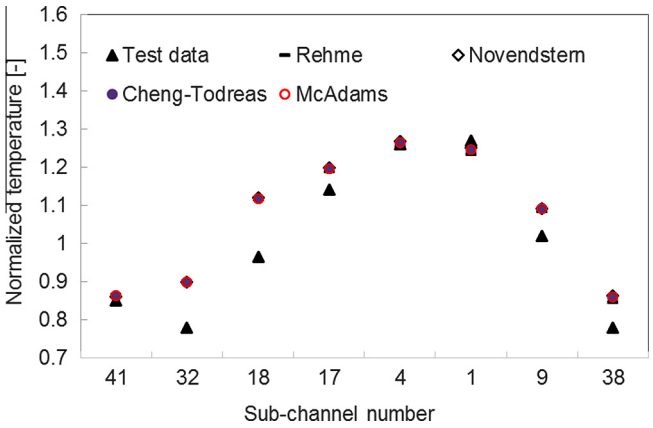

Fig. 13. Normalized temperatures at the end of the heated length (turbulent mixing model Cheng-Tak).

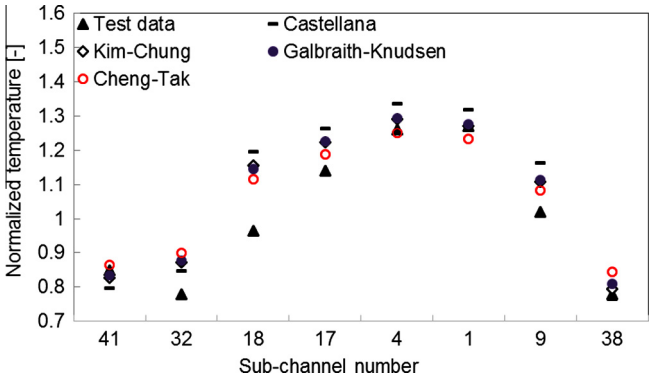

Fig. 14. Effect of turbulent mixing model on normalized temperatures (pressure drop model Rehme).

4.2. Cladding temperatures

The design of a LMR needs accurate predictions of the peak temperatures of the rod and coolant in order to decide safety and economic issues. The heat transfer models intervene in the calculation of the rod temperatures. Since the cladding temperature poses a major constraint in the design, it is very important to achieve a precise estimation, thus reliable heat transfer description is needed.

Due to the lack of benchmark data, the implementation of the models in COBRA-LM is based on a conservative approach and on the intrinsic reliability of the correlations. Another open calculation is performed, in order to underline the influence of the heat transfer toward the thermal-hydraulic analysis of the sub-channels.

As expected, the hot-spot occurs in the inner sub-channels, e.g., the central rod of the bundle. Fig. 15 shows Rod 1 cladding temperature profile computed with Rehme and Cheng-Tak models, but by different heat transfer correlations. The cladding temperature at the outlet of the assembly (without heating) is the same to the fluid temperature for all the simulations due to using the same turbulent mixing model. From the results it can be seen that Sleicher heat transfer coefficient provided temperature predictions similar to the Seban–Shimazaki correlation, while Graber model, due to the higher estimation of the Nusselt number, provides the lowest cladding temperature.

In order to investigate the influence of the flow characterization upon heat transfer, calculations are performed for fixed heat transfer correlation by varying either pressure drop or turbulent mixing model. Fig. 16 depicts the sensitivity of Kirillov-Stromquist heat transfer model with regards to Galbraith-Knudsen mixing coefficient for different the pressure drop models. Fig. 17 shows the sensitivity of Kirillov-Stromquist heat transfer models with regards to Cheng-Todreas pressure drop model by varying turbulent mixing correlations. Both temperature profiles are referred to the central fuel rod.

It is clear that the turbulent mixing plays a role in flattening the temperature distribution among sub-channels. In the framework of the ORNL 19-pin tests, it is even more important, together with the

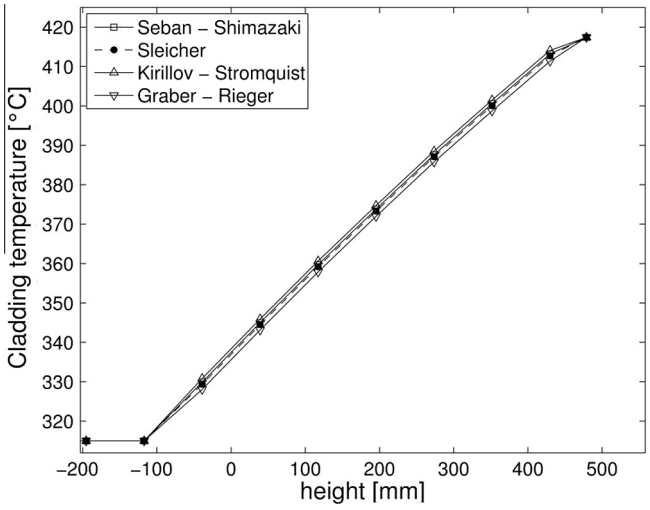

Fig. 15. Cladding temperature profile – Sensitivity on heat transfer models.

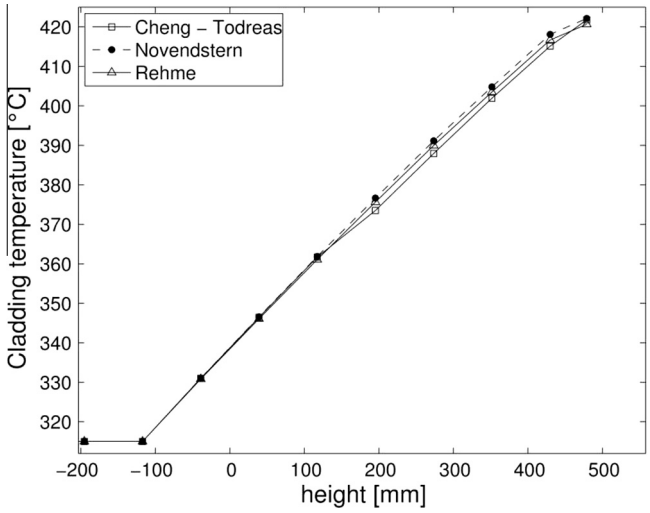

Fig. 16. Cladding temperature profile – Sensitivity on pressure drop models.

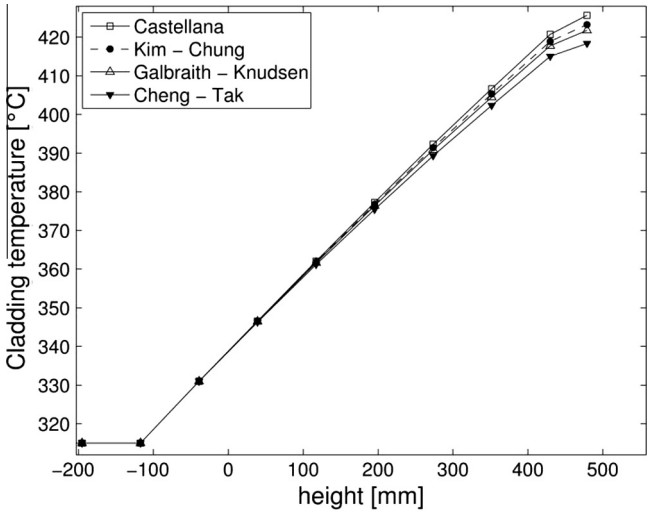

Fig. 17. Cladding temperature profile – Sensitivity on mixing models.

pressure drop, in determining the outlet temperature of the coolant. In fact, the top part of the bundle is not heated; in this conditions, referring to the same axial region, the larger is the mixing coefficient, the more energy is spread along the radial direction. It contributes to a temperature increase of the outer channels and a decrease in the inner ones.

4.3. Effect on the wire wrap modeling

To analyze the modeling effect of the wire wrap on the results, several simulations are performed to achieve the mass flux distribution and normalized temperature in typical sub-channels. The pressure drop model is Rehme correlation and turbulent mixing coefficient is Cheng-Tak correlation. According to the previous study for wire wrap (Steward et al., 1977), the specifies the lateral flow where wires wraps cross a gap as a function of the wrap pitch and axial flow rate is one important parameter. Therefore, in this study, several values (0.003, 0.025, 0.041, and 0.063) of this fraction are applied for sensitivity study.

Fig. 18 shows the normalized temperature of sub-channels with various crossflow fraction caused by wire wrap. It can be clearly found that the normalized temperature in the external

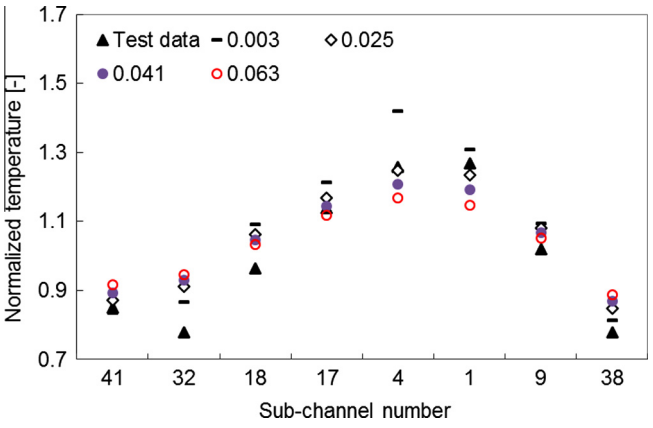

Fig. 18. Normalized temperature with various cross-flow fraction .

sub-channels (side and corner) increases with enhancing crossflow fraction caused by wire wrap, whereas the internal sub-channels show an opposite tendency. This is because the hot channels locate in the center of the bundle, where has a higher equivalent heating diameter. The results achieved demonstrate the crossflow effect due to wire wrap should be considered in the sub-channel analysis. It should be noted that this crossflow value varies strongly according to the location and geometry of different sub-channels. This is an important issue for the future study in the sub-channel analysis.

5. Sub-channel analysis for PHENIX reactor bundle

To demonstrate the applicability of the COBRA-LM code, the PHENIX reactor bundle simulation is performed (Tenchinea et al.,

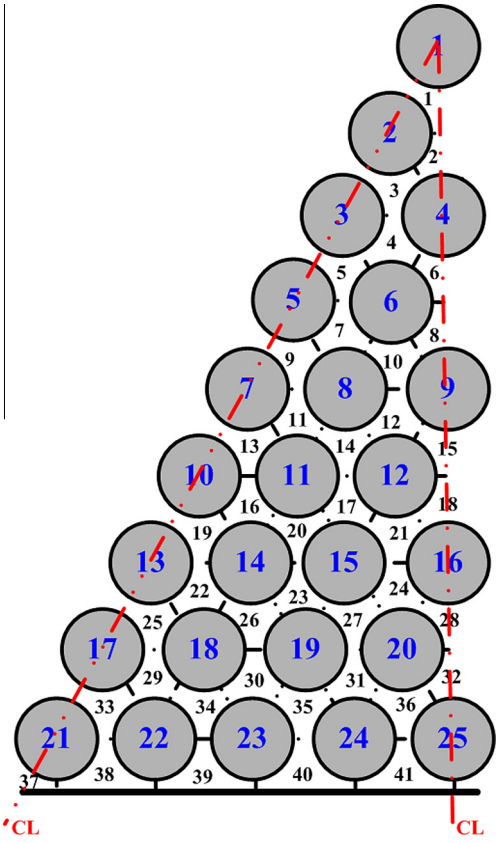

Fig. 19. Scheme of sub-channel and fuel rod in 1/12 fuel bundle.

Table 5
Summary of the parameters of inner bundle in Phenix reactor.

	Value
Geometry data	
Rod diameter (mm)	13.4
Pitch to diameter ratio (–)	1.08
Wire wrap diameter (mm)	1.08
Wire wrap pitch (mm)	200.0
Heating length (mm)	5365
Operation data	
System pressure (Pa)	10132.0
Inlet temperature (°C)	385.0
Outlet temperature(°C)	550.0
Inlet mass flux (kg/m^2-s)	3469.0
Average heat flux (kW/m^2)	882.0
Axial power distribution	Uniform
Radial power distribution	Uniform

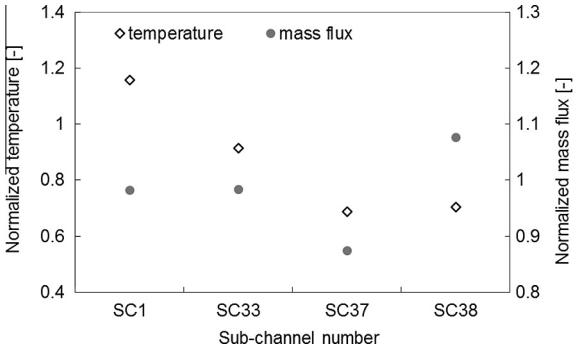

Fig. 20. Temperature and mass flux in typical sub-channels.

2013). Due to symmetry of the bundle, 1/12 of the bundle are analyzed. Fig. 19 shows the distribution and numbering of the sub-channels and fuel rods. Table 5 summaries the geometry and operation parameters of the PHENIX. The Rehme, Cheng-Tak and Sleicher correlation are utilized for pressure drop, turbulent mixing and heat transfer model respectively.

Fig. 20 shows the normalized mass flux and temperature of the typical sub-channel (SC 1, SC 33, SC 37, SC 38). It can be clearly to see the normalized temperature decreases from the center to the peripheral sub-channel. This can be caused by two effects: larger ratio of heated perimeter to wetted perimeter in the internal channels, and the heat transfer between the hot channels (in the center) to the cold channels (at peripheral). As for the mass flux factor, it is directly proportional to its hydraulic diameter, so the corner sub-channel 37 shows the lowest mass flux (SC 37 has the smallest hydraulic diameter).

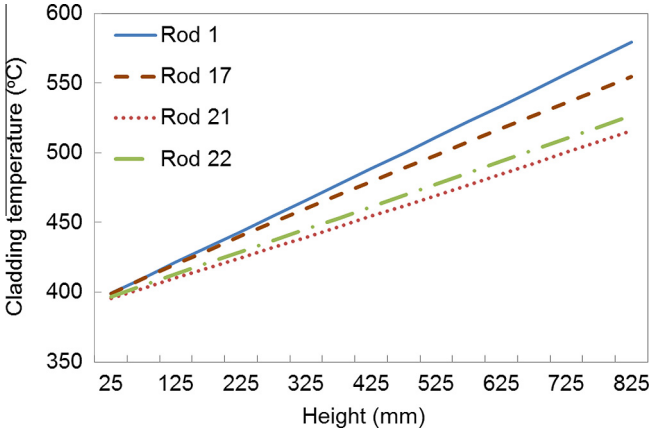

Fig. 21. Cladding temperature of typical fuel rods.

Fig. 21 presents the cladding temperature distributions of rod 1, rod 17, rod21 and rod 22, which stands for the internal, external, side and corner fuel rod respectively. Due to the temperature distribution in sub-channel shown in Fig. 20, the cladding temperature increases from the outer side to the center side of the bundle. The results achieved so far indicates that the new developed code COBRA-LM has good feasibility to the thermal-hydraulic analysis of the liquid metal cooled fuel assembly.

6. Conclusion and future work

The development of a sub-channel analysis code COBRA-LM for liquid metal cooled rod bundles was set up through adaptation of an existing code for LWRs. It represents a powerful way to develop more advanced models for sub-channel analysis. The assessment of COBRA-LM code was carried out by benchmark calculations involving CFX results, MATRA-LMR and experimental data from ORNL 19-pin tests. The comparison showed good agreement of the results in terms of normalized temperatures at the end of the heated length. Furthermore, a sensitivity analysis was performed in order to investigate the reliability of the physical models implemented in the sub-channel code. In this way, the features of heat transfer mechanism, pressure drop and turbulent mixing correlations were investigated and tested through a particular experimental configuration. The influence of the models on each other was studied by open calculations toward the definition of a particular set of correlations. This set was meant to provide the closest results to the experimental data from ORNL 19-pin tests. It is important to remark that this combination of models (Rehme model for pressure drop, Cheng-Tak correlation for turbulent mixing coefficient) was the most suitable to describe the configuration adopted as benchmark.

Much emphasis was put on the turbulent mixing and wire wrap crossflow models as they affect the temperature distributions to a large extent. Eventually, a sub-channel analysis for PHENIX reactor bundle is simulated by COBRA-LM code to show the code's applicability to liquid metal cooled bundles.

In the future, more investigation toward crossflow and mixing models development is needed, especially for liquid metal flows. The geometry effect (e.g., p/d ratio, sub-channel configuration) on the crossflow and mixing should be taken into account, since the strong empirical background the models are based on poses large uncertainties over results. It should be noted that the validation of the modified code for bundle geometry from LBE, is highly required in the future work.

Acknowledgement

This work is supported by Doctoral Fund of Ministry of Education of China (20110073120045).

References

Cheng, X., Tak, N.I., 2006. CFD analysis of thermal-hydraulic behavior of heavy liquid metals in sub-channels. Nucl. Eng. Des. 236, 1874–1885.
Cheng, S.K., Todreas, N.E., 1986. Hydrodynamic models and correlations for bare and wire-wrapped hexagonal rod bundles-bundle friction factor, Subchannel friction factors and mixing parameters. Nucl. Eng. Des. 92, 227–251.
Cheng, X., Batta, A., Chen, H.Y. et al., 2004. Turbulent heat transfer to heavy liquid metals in circular tubes, ASME Heat transfer/Fluids engineering Summer Conference, Charlotte, North Carolina.
Chun, M.H., Seo, K.W., 2001. An experimental study of pressure drop correlations for wire-wrapped fuel assemblies. KSME Int. J. 15 (3), 403–409.

Dobson, G.P., O'Neill, J.M., 1992. SABRE, User Guide for Version 4, RSSD 261, AEA Technology.

Fontana, M.H., Gnadt, P.A., MacPherson, R.E., et al., 1974. Temperature distribution in the duct wall and at the exit of a 19-rod simulated LMFBR fuel assembly (FFM Bundle 2A). Nucl. Technol. 24, 176–200.

Gen IV Roadmap, 2002. US DOE nuclear energy research advisory committee and the Generation IV international forum. A technology roadmap for generation IV nuclear energy systems. GIF002-00, December 2002. http://gif.inel.gov/roadmap/.

George, T.L., Basehore, K.L., Wheeler, C.L. et al., 1980. COBRA-WC: A version of COBRA for single-phase multiassembly thermal hydraulic transient analysis, Pacific Northwest Laboratory.

Gräber, H., Rieger, M., 1972. Experimentelle untersuchung des wärmeübergangs an flüssigmetall (NaK) in parallel durchströmten rohrbündeln bei konstanter und exponentieller wärmeflussdichteverteilung. Atomkernenergie 19, 23–40.

Jeong, H.Y., Ha, K.S., Kwon, Y.M., et al., 2007. A dominant geometrical parameter affecting the turbulent mixing rate in rod bundles. Int. J. Heat Mass Transfer 50, 908–918.

Kim, W.S., Kim, Y.G., Kim, Y.J., 2002. A Subchannel analysis code MATRA-LMR for wire-wrapped LMR subassembly. Ann. Nucl. Energy 29 (2002), 303–321.

Kirillov, P.L., Ushakov, P.A., 2001. Heat transfer to liquid metals: specific features, methods of investigation and main relationships. Therm. Eng. 48 (1), 50–59.

Novendstern, E.H., 1972. Turbulent flow pressure drop model for fuel rod assemblies utilizing a helical wire wrap spacer system. Nucl. Eng. Des. 22, 19–27.

Rehme, K., 1972. Pressure drop correlations for fuel element spacers. Nucl. Technol. 17, 15–23.

Seban, R.A., Shimazaki, T.T., 1951. Heat transfer to a fluid flowing turbulently in a smooth pipe with walls at constant temperature. Trans. ASME 73, 803–809.

Sobolev, V., 2010. Database of thermophysical properties of liquid metal coolants for GEN-IV, SCK-CEN Boeretang 200 2400, Mol, Belgium.

Steward, C.W., Wheeler, C.L., Cena, R.J., 1977. COBRA-IV: the model and the method. In: Battelle Pacific Northwest Laboratories Richland, Washington, USA.

Stromquist, W.K., Boarts, R.M., 1953. Effect of wetting on heat transfer characteristics of liquid metals. University of Tennessee, ORO-93.

Tenchinea, D., Piallaa, D., Fanningb, T.H., et al., 2013. International benchmark on the natural convection test in Phenix reactor. Nucl. Eng. Des. 258, 189–198.

Wu, Y.W., Li, X., Yu, X.L., et al., 2013. Subchannel thermal-hydraulic analysis of the fuel assembly for liquid sodium cooled fast reactor. Prog. Nucl. Energy 68, 65–78.

Yang, W.S., 1997. An LMR core thermal-hydraulics code based on the ENERGY model. J. Korean Nucl. Soc. 29, 406–416.